Weak interaction physics at ISOLDE

2017 J. Phys. G: Nucl. Part. Phys. 44 074002

(http://iopscience.iop.org/0954-3899/44/7/074002)

IOP Publishing Journal of Physics G: Nuclear and Particle Physics
J. Phys. G: Nucl. Part. Phys. **44** (2017) 074002 (24pp) https://doi.org/10.1088/1361-6471/aa71e3

Weak interaction physics at ISOLDE*

N Severijns[1,3] and B Blank[2]

[1] KU Leuven, Department of Physics and Astronomy, Instituut voor Kern- en Stralingsfysica, Celestijnenlaan 200 D, B-3001 Leuven, Belgium
[2] CEN Bordeaux-Gradignan, 19 Chemin du Solarium, CS 10120, F-33175 Gradignan, France

E-mail: nathal.severijns@fys.kuleuven.be and blank@cenbg.in2p3.fr

Received 1 January 2017, revised 20 March 2017
Accepted for publication 9 May 2017
Published 6 June 2017

Abstract

Radioactive nuclei offer unique possibilities to study the structure and symmetries of the weak interaction in nuclear β decay. The large variety of nuclear states available allows selecting the ones that are best suited to study the phenomena of interest with optimal sensitivity, while at the same time minimising the effects of nuclear structure. The ISOLDE facility, offering worldwide the largest variety and intensity of radioactive beams, is one of the best suited laboratories in this respect. Over the last decade or so different aspects of the weak interaction have been studied at ISOLDE, ranging from half-lives, branching ratios and nuclear masses relevant for the determination of the V_{ud} quark-mixing matrix element, over β-asymmetry and $\beta\nu$ correlation measurements searching for possible tensor and/or scalar contributions to the weak interaction, up to a measurement showing the effect of parity violation in the weak interaction in gamma decay. In addition, new projects respectively searching for scalar currents in the β-delayed proton decay of ^{32}Ar, or to determine the V_{ud} quark-mixing matrix element from the β-asymmetry parameter in the mirror decay of ^{35}Ar, have just started.

Keywords: weak interaction, nuclear beta decay, $\mathcal{F}t$-values, tensor currents, scalar currents, parity violation

(Some figures may appear in colour only in the online journal)

1. Introduction

Nuclear beta decay has made some very important contributions to our present understanding of the weak interaction, for example establishing the violation of parity [1, 2], the helicity of

* This article belongs to the Focus on Exotic Beams at ISOLDE: A Laboratory Portrait special issue.
[3] Author to whom any correspondence should be addressed.

the (anti)neutrino [3], the vector–axial-vector (V–A) structure of the weak interaction [4], and the V_{ud} quark-mixing matrix element (e.g. [5]). Correlation measurements between the spin and momentum vectors of the particles involved in nuclear β decay have over the years refined our understanding of the V–A structure (thereby e.g. providing limits on possible scalar and tensor type contributions), and have allowed for precise tests of the parity and time reversal symmetries in the weak interaction (for reviews see [6–15]; reviews on related results from experiments in free neutron decay can be found in e.g. [16, 17]).

Whereas in collider experiments, for example the *Large Hadron Collider* (LHC), one can try to directly produce possible new gauge bosons, at low energies such as in nuclear β decay, one searches for the small deviations such new bosons cause to the Standard Model values of unambiguously predicted observables. Previously it has been shown already that both approaches probe complementary parameter regions when interpreted in more general extensions of the Standard Model [18]. Recently, a unified effective field theory framework based on a quark-lepton level effective Lagrangian [13, 19, 20] was put forward. Assuming the new physics to emerge only at an energy scale well above the production threshold of the LHC (such that experiments at the LHC can in fact also be considered to be 'low-energy' experiments) results from β decay and searches at the LHC can be compared in a rather model-independent way. It was shown [11, 13, 21, 22] that low- and high-energy searches for new CP-conserving scalar and tensor interactions involving left-handed neutrinos are competitive and remain so even after the energy and intensity upgrades of the LHC if precisions of the order of 10^{-3} are reached for the Fierz interference term [23] in nuclear decays and neutron decay.

Experiments in nuclear β decay can take advantage of the huge variety of ground and excited states that are available to select both the isotope and the β transition such as to obtain optimal sensitivity to the physics being investigated, with minimal or no disturbance from effects related to nuclear structure. E.g. for isotopes at or near the $N = Z$ line nuclear structure is often sufficiently well known to not limit the sensitivity while, in addition, measurements on pure Fermi (F) or Gamow–Teller (GT) transitions render results independent of the nuclear matrix elements. Also, measurements of a particular observable can be performed with different isotopes thereby providing important cross-checks.

Over the last about two decades significant progress in precision was made in nuclear β decay experiments (e.g. [24–30]) using a variety of new techniques, such as atom traps [31] and ion traps [32], as well as new and advanced Geant4-based simulation codes performing well at β-particle energies (e.g. [35, 33, 34, 36]).

Recent experiments at ISOLDE have contributed to many aspects of probing the properties of the weak interaction: (i) precision decay spectroscopy on super-allowed pure Fermi decays [5] and mirror β transitions [37, 38], as well as high-precision mass measurements taking advantage of the excellent (up to the 10^{-9} level) precision that can be reached with Penning trap based mass spectrometers [32] such as ISOLTRAP [39], have been performed, all contributing to the determination of the V_{ud} quark-mixing matrix element, (ii) a measurement of the beta emission asymmetry parameter in the decay of ^{67}Cu [36] polarised with the low-temperature nuclear orientation method [40, 41] was performed, providing information on the possible presence of a tensor type contribution to the weak interaction, while (iii) the WITCH experiment has been trying to search for a scalar type contribution [42–44], and (iv) a measurement of the anisotropy of γ rays in the decay of oriented ^{180m}Hf [45] has confirmed and extended the evidence for parity violation in the γ decay of this isomeric state. Finally, a series of other experiments is ongoing or being set up, for example a measurement of the β-asymmetry parameter in the decay of collinear laser beam polarised ^{35}Ar [46], and of the $\beta\nu$ correlation in the β-delayed proton decay of ^{32}Ar [48].

2. Precision decay spectroscopy and nuclear mass measurements

The V_{ud} matrix element of the Cabibbo–Kobayashi–Maskawa quark-missing matrix can be determined experimentally by three different means: (i) pion decay, (ii) nuclear mirror β decays, the neutron decay being one particular mirror decay, and (iii) super-allowed β decay of the $0^+ \rightarrow 0^+$ type. The super-allowed β decays give by far the best precision (2×10^{-4}) for V_{ud} [5], with mirror decays [37, 38], neutron decay [50] and pion decay [51, 52] yielding about one order of magnitude lower precision. To achieve this precision in super-allowed and mirror decays, the cases of interest in the present paper, the conservation of the vector current (CVC) at the origin of these decays has to be verified. This is done via the constancy of the so called 'corrected $\mathcal{F}t$ value', which then allow the extraction of their average. For super-allowed $0^+ \rightarrow 0^+$ decays, this corrected $\mathcal{F}t$ value is linked to the vector coupling constant as follows [5]:

$$\mathcal{F}t = f_{\mathrm{V}}\, t\,(1 + \delta'_{\mathrm{R}})(1 + \delta_{\mathrm{NS}} - \delta_{\mathrm{C}}) = \frac{K}{G_{\mathrm{V}}^2 \langle M_{\mathrm{F}} \rangle^2 (1 + \Delta_{\mathrm{R}}^{\mathrm{V}})},$$

where f_{V} is the statistical rate function for the vector part of the interaction depending on Q_{EC}, the energy release of the transition. t is the partial half-life and is equal to $T_{1/2}(1 + P_{\mathrm{EC}})/\mathrm{BR}$, $T_{1/2}$ being the half-life of the parent nucleus, BR the branching ratio of interest and P_{EC} the probability of electron capture [5]. δ_{NS} is a nuclear structure dependent radiative correction and δ_{C} is the isospin symmetry breaking correction. δ'_{R} and $\Delta_{\mathrm{R}}^{\mathrm{V}}$ are the transition-dependent and transition-independent parts of the radiative corrections, respectively. These corrections are determined theoretically by models (see [5, 37] for details). K is a constant and $\langle M_{\mathrm{F}} \rangle$ is the Fermi matrix element which is equal to $\sqrt{T(T+1) - T_{\mathrm{zi}} T_{\mathrm{zf}}}$, where T is the isospin of the decaying nucleus and T_{zi} and T_{zf} are the isospin projections for the initial and final states, respectively.

Experimentally, the β-decay half-life, the super-allowed branching ratio and the decay Q value, the difference between the masses of the parent state and the analogue state in the daughter nucleus, have to be measured. Currently, fourteen super-allowed Fermi transitions between ^{10}C and ^{74}Rb are used to determine the average $\mathcal{F}t$ value.

Contrary to $0^+ \rightarrow 0^+$ decays which are pure Fermi decays, nuclear mirror β decays are mixed Fermi and GT transitions for which the $\mathcal{F}t$ value is no longer constant. However, a constant can be defined by taking this mixing into account:

$$\begin{aligned}\mathcal{F}t_0 &= f_{\mathrm{V}}\, t \left(1 + \frac{f_{\mathrm{A}}}{f_{\mathrm{V}}}\rho^2\right)(1 + \delta'_{\mathrm{R}})(1 + \delta_{\mathrm{NS}} - \delta_{\mathrm{C}}) \\ &= \frac{K}{G_{\mathrm{V}}^2 \langle M_{\mathrm{F}} \rangle^2 (1 + \Delta_{\mathrm{R}}^{\mathrm{V}})},\end{aligned}$$

f_{A} is the statistical rate function for the axial-vector part of the interaction, and ρ is the mixing ratio of Fermi and GT transitions [38]. Five mirror transitions ranging from ^{19}Ne to ^{37}K are available to determine $\mathcal{F}t_0$.

The results for $\mathcal{F}t$ and $\mathcal{F}t_0$ are based on about 180 original experimental papers for the super-allowed $0^+ \rightarrow 0^+$ decays and about 40 for the half-life and branching ratio measurements for the mirror decays, the Q values for these decays being taken from the Atomic Mass Evaluation [53].

Once the average of the $\mathcal{F}t$ and $\mathcal{F}t_0$ values are obtained, the vector coupling constant can be determined and from it the V_{ud} matrix element by means of the following expression:

$$V_{ud} = \frac{G_V}{G_\mu},$$

where G_μ is the coupling constant of the purely leptonic muon decay [49, 54].

A significant number of measurements for this purpose has been performed at ISOLDE. For the mass and Q-value measurements, the ISOLTRAP Penning trap mass spectrometer [55] has been used, whereas for half-life and branching ratio measurements 'travelling set-ups' were used, i.e. set-ups which were mounted at ISOLDE for the purpose of one experiment and dismounted afterwards. In the following sections we will describe these experiments.

2.1. Half-life and branching ratio measurements

For half-life and branching ratio measurements, the production capabilities of ISOLDE for $0^+ \rightarrow 0^+$ or mirror decays have been used little up to now. Only the results for two nuclei, ^{38,39}Ca, are published as of today. The results for one additional nucleus, ^{37}K, are published in the present special issue. For the former two nuclei, the half-lives have been determined with high precision, whereas for the latter half-life and branching ratios were obtained. In addition, the data of a branching ratio experiment for ^{10}C are presently being analysed.

2.1.1. Half-life of ^{38,39}Ca. ^{38}Ca is one of the heavier $T_z = -1$ nuclei presently accessible for high-precision measurements. These nuclei are of interest, not necessarily because a very high precision can be reached, but rather to test the theoretical isospin symmetry breaking correction, δ_C, mentionned above. Indeed the overall precision achievable for these $T_z = -1$ nuclei is limited by the precision which can be obtained for the branching ratio. These nuclei have rather high non-analogue, i.e. non $0^+ \rightarrow 0^+$, transitions which requires high-precision γ-ray spectroscopy measurements with germanium detectors. However, efficiency calibrations of these detectors are typically limited to 0.1% precision [56, 57], which limits the precision on the branching ratio and thus the overall precision for the corrected $\mathcal{F}t$ value to typically 0.1%–0.2%.

To prepare the ultra-pure samples for the half-life measurements of the present experiment, a titanium-foil target was bombarded by the PS Booster proton beam with an intensity of 2.0–2.7 $\times$ 10^{13} protons per pulse [58]. A fluorine leak in the target—ion-source ensemble allowed the production of CaF^+ molecules and the separation of calcium isotopes, by means of the ISOLDE high-resolution mass separator HRS, from the much more abundant potassium isotopes which do not form KF molecules in a 1^+ charge state. The CaF^+ molecular ions were accumulated in the REXTRAP Penning trap facility. After accumulation, the trap was opened and the bunch of molecules and ions was ejected towards a tape station (see figure 1). This ejection allowed a time-of-flight analysis and only mass $A = 57$ or $A = 58$ molecules were accumulated on the tape for the ^{38}Ca and ^{39}Ca measurements, respectively [59].

The half-life measurements were performed in cycles of accumulation in REXTRAP (typically 600 ms), tape transport from the accumulation point to the measurement position (265 ms), and decay measurement (7.5 s). A total of 1.2 $\times$ 10^6 ^{38}Ca decays were registered. For ^{39}Ca, a total of 2.5 $\times$ 10^6 decays were measured.

Figure 2(a) shows a typical decay-time spectrum for ^{38}Ca. The decay curve is composed of the decay of ^{38}Ca and the grow-in and decay of ^{38}K, the daughter nucleus. In figure 2(b), we show the results obtained for the half-life as a function of the run number. The results for the different runs, registered with different experimental parameters (see [58] for details), yield statistically compatible results with a final half-life value of $T_{1/2} = 443.9(19)$ ms.

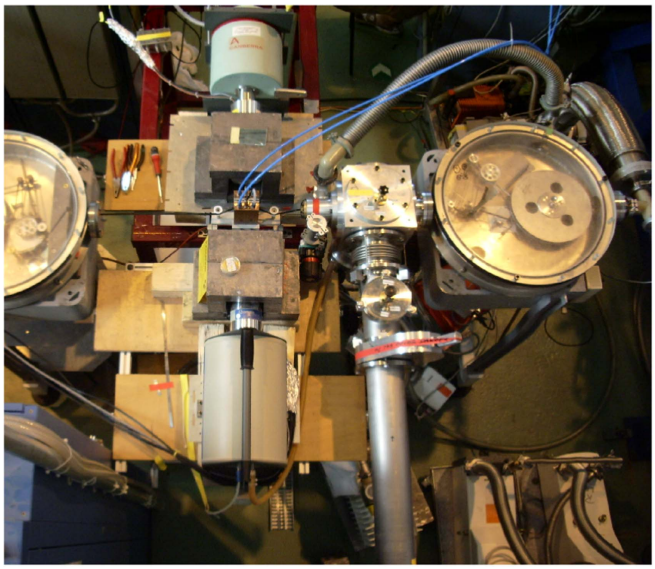

Figure 1. Experimental setup used of the measurement of the half-lives of ^{38,39}Ca. On the right is the beam pipe where the nuclei of interest arrive. In the chamber at the end of this beam pipe, they are deposited on a tape which transports them to the measurement position in the centre of two half-sphere of Geiger counters and the two germanium detectors shielded by lead bricks. On the left and the right, the two wheels of the tape transport system is seen.

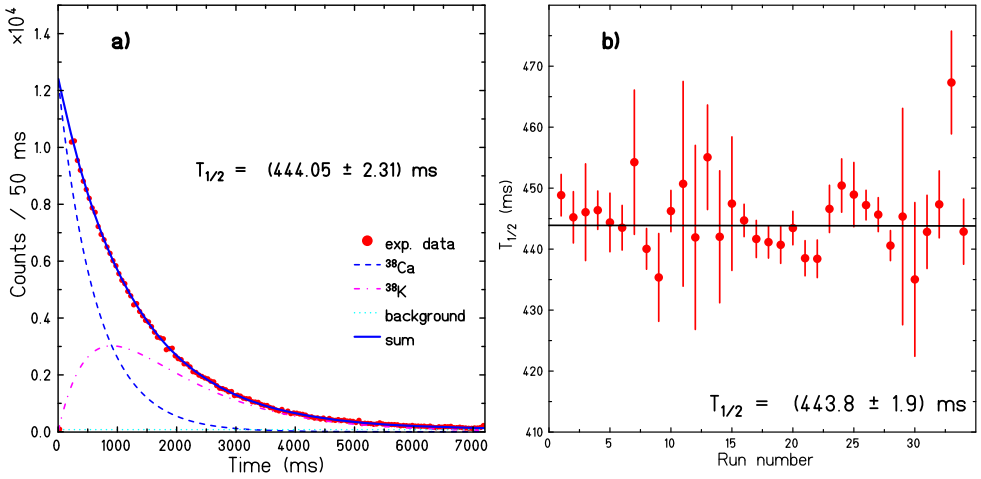

Figure 2. (a) ^{38}Ca half-life spectrum from one run yielding a half-life of 444.05 (231) ms. The full points are the experimental data. The different lines show the different contributions to the spectrum. (b) The half-life values determined for the different runs are shown together with the average value yielding the final half-life. [58] (2010) (© SIF, Springer-Verlag Berlin Heidelberg 2010). With permission of Springer.

At the time of the measurement and publication, this result was four times more precise than the average of all previous measurements. In the mean time, measurements performed at Texas A&M ($T_{1/2}$= 443.77(36) ms) [60] and at GANIL ($T_{1/2}$= 443.63(35) ms) [61] improved

the precision on the half-life significantly due to higher-statistics experiments. The present world average is $T_{1/2} = 443.70(25)$ ms with a precision of 0.05%.

In these experiments, the super-allowed branching ratio was also measured to be 77.28 (16)% [62] and 77.14(35)% [61] yielding an average value of 77.25(15)%. As the mass excess values have been measured at ISOLTRAP (see below) and at Michigan State University, all experimental parameters to determine the corrected $\mathcal{F}t$ are presently available, yielding $\mathcal{F}t = 3077.5(67)$ s. For the reasons mentioned above, this value is limited by the precision of the branching ratio measurements.

The half-life of ^{39}Ca was determined to be 860.7(10) ms. This value agrees with the previously measured half-life values and gives a total average of 860.6(8) ms with a precision of 0.09%.

The branching ratio of this nucleus is known with a precision of 2×10^{-6} (BR = 99.9975(2)%) and its Q value is $Q_{EC} = 6532.61(19)$ keV. Both results, like the half-life, are well enough known to contribute to the test of the CVC hypothesis and the determination of V_{ud}, once the Gamow–Teller to Fermi (GT/F) mixing ratio is measured. Plans for these measurements exist at GANIL [63].

2.1.2. Half-life and branching ratio of ^{37}K. The measurements performed for this nucleus are published in the present issue as a contribution [64]. Therefore, we refrain from giving details about this measurement here. The half-life determined is $T_{1/2} = 1.236\,35(88)$ s and the most important non-analogue branching ratio is BR = 2.20(17)%. The present measurement of the half-life is in agreement with a measurement from Texas A&M [65] recently published yielding, together with all literature value a new world average of 1.236 34(64) s. The world average for the super-allowed branching ratio is now BR = 97.96(14)%.

With the Q value already precisely known ($Q_{EC} = 6147.46(20)$ keV), the limiting factor of the experimental quantities is the GT/F mixing ratio. ^{37}K being one of the five nuclei for which this mixing ratio is known, its uncertainty is nonetheless of the order of 4% (see figure 3). However, as potassium is an element relatively easy to produce at ISOL facilities, an experiment could be designed to improve this experimental quantity.

2.1.3. Branching ratio of ^{10}C. The super-allowed branching ratio of ^{10}C, the lightest of all super-allowed β emitters, was measured several times in the past, however, only twice with high precision. In both cases, the measurement was performed with a multi-detector germanium array [66, 67]. The ^{10}C activity was produced by a ^{10}B(p, n)^{10}C reaction in a thick target. The precise γ-detection efficieny was obtained by populating the states of interest by the reaction ^{10}B(p, p)^{10}B (see figure 4) by gating on the 414.1 keV γ ray and determining thus the relative efficiencies for the 718.3 and 1021.7 keV γ rays of interest.

Evidently, the tricky part in the determination of the super-allowed branching ratio for this nucleus is to correctly take into account the pile-up of two 511 keV annihilation quanta with respect to the 1021.7 keV γ ray from the ^{10}C decay. A multi-detector array minimises this problem because each individual detector has a modest efficiency and thus also a small pile-up probability, however, due to the number of detectors (20 in [66] and 47 in [67]), a large overall efficiency is obtained.

In an ISOLDE experiment, a different approach was used. A precisely efficiency-calibrated germanium detector [57] was used to measure the relative intensities of the 718.3 and 1121.7 keV γ rays. In order to determine correctly the pile-up probability, ^{19}Ne decay was used taking profit from the fact that this nucleus has a half-life and a β-decay Q value close to ^{10}C. Therefore, the pile-up probabilities in both cases should be similar, with ^{19}Ne not having a γ ray at 1022 keV. Therefore, all events in this region come from pile-up, and once the pile-up rates are understood for ^{19}Ne, the ^{10}C decay can be corrected for in the same way.

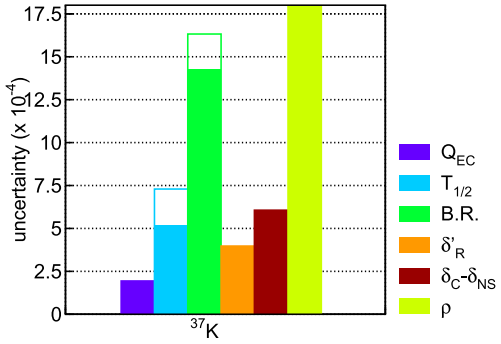

Figure 3. Uncertainty budget for the corrected $\mathcal{F}t$ value of ^{37}K. All parameters are known with a precision of 0.15% or better (full boxes), except for the mixing ratio, ρ, which has an uncertainty of about 4% (out of scale in the present representation). The open boxes give the uncertainties before our ISOLDE experiment.

In addition, the shaping times of the γ-ray signals were changed (1 and 2 μs), the beam intensity was varied widely (from taking every second proton pulse from the PS Booster for the highest rates to taking only one proton pulse out of six), and the distance between the ^{10}C source and the germanium detector was changed (15 and 20 cm).

All these different experimental conditions have to yield compatible results. The data are presently being analysed.

2.2. Mass excess and Q value measurements with ISOLTRAP

As mentioned above, beyond the half-life and the super-allowed branching ratio also the decay Q value has to be determined. A lot of these Q values have been measured by Penning-trap mass spectrometry with precisions of the order of 1 keV or better. The best precision is in general reached by measuring in the same experiment the mass of the parent and the daughter nucleus, usually by alternating between the two measurements within a short time. Thus, apart from magnet field drifts, temperature and pressure dependent effects, the mass-dependent systematic uncertainties are much smaller than the statistical ones in this type of measurement and the Q value is obtained directly from the frequency ratio. However, sometimes only one of the two masses is measured and literature data have to be used to obtain the Q value of interest.

2.2.1. Mass measurements of $0^+ \rightarrow 0^+$ emitters. ISOLTRAP has contributed to the precise knowledge of the Q value of two $T_z = 0$ nuclei, ^{26}Al^m [68] and ^{74}Rb [69], and to four $T_z = -1$ nuclei, ^{18}Ne [70], ^{22}Mg [71], ^{34}Ar [55, 72], and ^{38}Ca [73]. In addition, the mass of one $T_z = -2$ nucleus, ^{32}Ar [74], was measured. Figure 5 shows a frequency measurement with the time-of-flight ion-cyclotron-resonance technique for the ^{22}Mg parent and the ^{22}Na daughter nuclei. The frequencies allow the determination of the Q value by means of the following formula:

$$Q = m_{\mathrm{p}} - m_{\mathrm{d}} = \left(\frac{\nu_{\mathrm{d}}}{\nu_{\mathrm{p}}} - 1\right)(m_{\mathrm{d}} - m_{\mathrm{e}}),$$

m_{p} and m_{d} are the parent and daughter mass excess values, m_{e} is the electron mass, and ν_{p} and ν_{d} are their cyclotron frequencies.

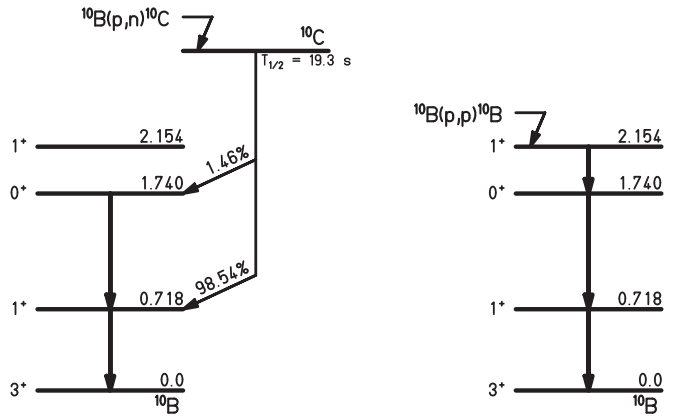

Figure 4. Left-hand side: decay scheme of ^{10}C produced in a ^{10}B(p, n)^{10}C reaction. Right-hand side: decay scheme of the excited state at 2.154 MeV populated in a ^{10}B(p, p)^{10}B reaction used to calibrate the set-ups in relative efficiency for the γ rays of interest at 718 keV and 1022 keV by gating on the 414 keV γ line. This approach has been used in previous high-precision measurements of the branching ratios.

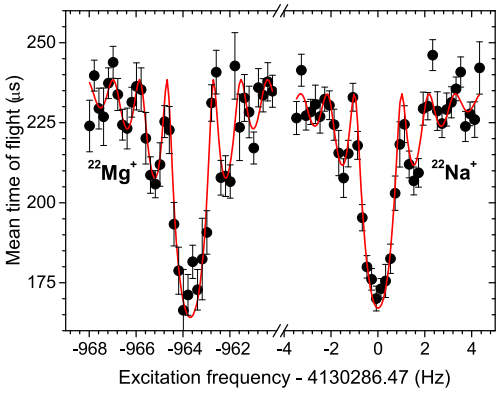

Figure 5. Cyclotron frequencies as determined by the time-of-flight ion-cyclotron-resonance technique with ISOLTRAP for the ^{22}Mg parent and the ^{22}Na daughter nuclei. Reproduced with permission from V. Manea.

The Q value of these super-allowed $0^+ \rightarrow 0^+$ decays is one of the few nuclear physics topics where a precision of 1 keV or below is required. Therefore, Penning-trap mass spectroscopy has to be pushed to its best performances for these studies. As some of the super-allowed emitters are relatively short-lived ($T_{1/2} = 65$ ms for ^{74}Rb) and the production rates are low, the measurements are challenging. Nevertheless, resolving powers of 10^6 are routinely reached resulting in mass and Q value precisions of 10^{-8} and better.

Table 1 gives details about the measurements performed with ISOLTRAP. For most of the cases, only the mass of the parent has been measured or the parent and the daughter mass have been determined in two independent measurement campaigns (^{74}Rb/^{74}Kr). Only in one case, ^{22}Mg, the Q value has been determined in a single measurement.

Today, 14 super-allowed $0^+ \rightarrow 0^+$ emitters are used to test the CVC hypothesis, to determine the vector coupling constant and the V_{ud} quark-mixing matrix element, ranging

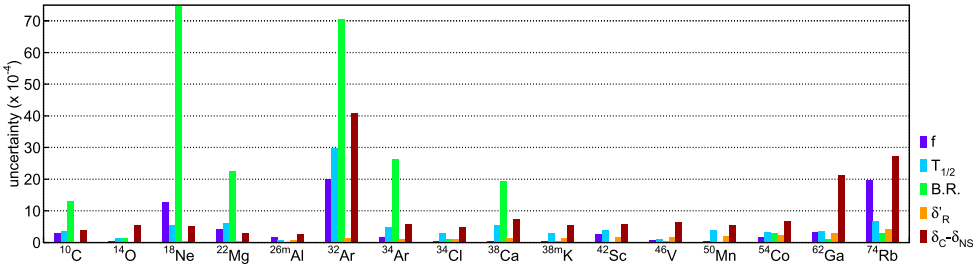

Figure 6. Uncertainty budget for 16 super-allowed $0^+ \rightarrow 0^+$ emitters ranging from ^{10}C to ^{74}Rb. The data include ^{18}Ne for which the ground-state mass excess was measured at ISOLTRAP. For this nucleus, a high-precision branching ratio measurement is still missing. Also added is ^{32}Ar ($T_z = -2$) for which the ground-state mass excess, the half-life and the branching ratio were measured at ISOLDE.

Table 1. Mass excess or Q value measurements performed with ISOLTRAP for $0^+ \rightarrow 0^+$ emitters. In one case, the Q value was directly measured, whereas in all other cases only the mass of the parent was measured or parent and daughter mass excess values were determined in independent measurements. The 'average Q value' is the value accepted today [5] which includes in some cases measurements performed after the ISOLTRAP measurements. The column 'limitation' indicates which problem limits today the precision of the Q value. In this context, 'inconsistencies' mean that different measurements disagree significantly.

Parent isotope	ISOLTRAP parent mass	ISOLTRAP Q value	Average Q value	Limitation
^{18}Ne	5317.63(36)		302.66(69)	Daughter mass
^{22}Mg		4781.64(28)	4124.53(28)	Q value
^{26}Al^m	−12 210.20(06)		4232.66(12)	Inconsistencies
^{32}Ar	−2200.2(1.8)		11134.8(20)	Parent mass
^{34}Ar	−18 377.10(41)		6061.87(19)	Inconsistencies
^{38}Ca	−22 058.01(65)		6612.12(7)	Parent mass
^{74}Rb	−51 915.2(40)		10 416.8(39)	Parent mass

from ^{10}C to ^{74}Rb (see figure 6). For all of them but ^{74}Rb, the Q value has been measured directly in a single experiment. In the case of ^{74}Rb, an improvement of the Q value would improve the overall precision of the $\mathcal{F}t$ value, as the Q value uncertainty is the second contributor to the uncertainty budget, almost as large as the nuclear-structure dependent theoretical correction (see figure 6).

The case of ^{32}Ar is particular in the sense that it is the only $T_z = -2$ nucleus for which a relatively high precision of all experimental parameters has been reached (see figure 6). The Q value (6087.3(22) keV) was obtained from a measurement of the mass excess of ^{32}Ar [74] at ISOLTRAP, from the mass excess of ^{32}Cl from a ^{32}S(^{3}He,t) reaction at the Maier-Leibnitz-Laboratorium of the Ludwig-Maximilians-Universität and the Technische Universität München [75], and from a mass excess determination with JYFLTRAP [76]. The super-allowed branching ratio was determined with a precision below 1% [77], including a strong decay branch by β-delayed proton emission. With the half-life from the same experiment ($T_{1/2} = 100.5(3)$ ms), the $\mathcal{F}t$ value was determined and the isospin symmetry correction δ_C was extracted and compared to shell model calculations. The experimental result, $\delta_C = 2.1$

Table 2. Mass excess measurements performed with ISOLTRAP for mirror decays. To determine the β-decay Q values, the mass excess values of the daughter nuclei (all stable, except for the case of ^{37}K) have to be used which are all rather well known.

Parent isotope	^{19}Ne [70]	^{21}Na [71]	^{37}K [78]	^{39}Ca [68]
Parent mass excess	1751.83 (31)	−2184.71 (21)	−24 800.45(35)	−27 282.57(60)

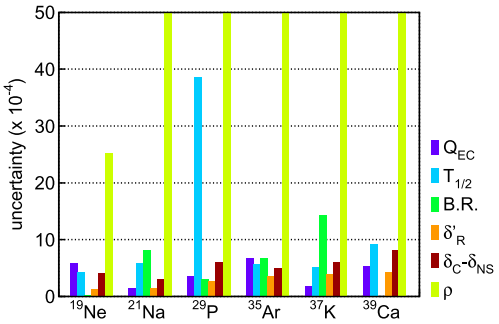

Figure 7. Uncertainty budget for the five mirror decays for which all experimental quantities are measured and for ^{39}Ca. For ^{21}Na, ^{29}P, ^{35}Ar, and ^{39}Ca, the error for the mixing ratios is out of scale. For ^{39}Ca, the mass excess was measured at ISOLTRAP, but no mixing ratio measurement exists.

(8)%, in agreement with the shell-model result, is larger than any other δ_C correction for the 14 super-allowed $0^+ \rightarrow 0^+$ emitters[4].

2.2.2. Q values of mirror decays. ISOLTRAP has contributed to the knowledge of the Q values of the mirror β decays of ^{19}Ne [70], ^{21}Na [71], ^{37}K [78], and ^{39}Ca [68]. The mass excess values measured are given in table 2. The precision of the mass excess was improved for ^{19}Ne by a factor of 2, for ^{21}Na by a factor of 3.5, and for ^{39}Ca by a factor of 3. The measurement of the mass excess of ^{37}K confirmed a previous measurement with a factor of 4 less precision.

For ^{19}Ne, ^{21}Na, and ^{37}K, all experimental parameters needed to determine the corrected $\mathcal{F}t_0$ value are known. Therefore, the increase in precision for the Q values for these nuclei was of particular interest (see figure 7). In none of the cases, the Q value is the limiting factor. For these mirror decays, by far the largest uncertainty comes from the GT/F mixing ratio. Even in the case of ^{19}Ne, where this ratio is best known, the next contributor to the uncertainty, the Q value, is a factor of 5 more precise. Therefore, in order to improve the overall precision of the corrected $\mathcal{F}t_0$ values for mirror decays, new measurements of the mixing ratio are needed for different nuclei.

2.3. Conclusion

ISOLDE had as significant contribution in the measurements of experimental inputs to determine the corrected $\mathcal{F}t$ and $\mathcal{F}t_0$ values, be it for the super-allowed $0^+ \rightarrow 0^+$ or the mirror decays. Experimental data have been obtained for mass excess and Q values as well as for

[4] In the work of [77], the nuclear-structure dependent radiative correction δ_{NS} was not yet introduced.

half-lives and branching ratios. Some of these data are still being analysed or published in the present special issue.

For the super-allowed decays of the $0^+ \rightarrow 0^+$ type, in particular the branching ratios of ^{18}Ne, ^{22}Mg, and ^{34}Ar, the limiting parameters for these nuclei, could be addressed in future measurements. For the β-decay Q values, it might be worth attempting again a measurement for ^{74}Rb.

In the case of the mirror decays, the situation is different. Here in all cases, the limiting parameter is the GT/F mixing ratio. Depending on the nuclei which will be considered for future measurements of this parameter, measurements of Q value, half-life and branching ratio could be envisaged at ISOLDE.

2.4. Outlook—extracting V_{ud} from the β asymmetry parameter of laser-polarised ^{35}Ar

Recently, a new project [46] started at ISOLDE aiming to determine the β-asymmetry parameter, A, in the $3/2^+ \rightarrow 3/2^+$ mirror β decay of ^{35}Ar to the ^{35}Cl ground state with an endpoint energy of 4.944 MeV and a branching ratio of 98.2%. It was shown [10] that when considering the $\beta\nu$ correlation and β-asymmetry parameter for the mirror β transitions a measurement of the β-asymmetry parameter, A, for ^{35}Ar provides the highest sensitivity to the quark-mixing matrix element V_{ud}. Indeed, a measurement of A with a relative precision of 0.5% would yield V_{ud} with an absolute uncertainty of 0.0007 [10], only a factor of about 3 worse than the value obtained from the weighted average $\mathcal{F}t$ value of the super-allowed pure Fermi β transitions [5]. Moreover, if the corrected $\mathcal{F}t$ value for ^{35}Ar is improved by a factor 5, the absolute uncertainty on V_{ud} could even be as low as 0.0004 [10]. This requires improvements of the Q_{EC} value, the branching ratio and the half-life for the mirror β transition of this isotope. Such measurements are planned at JYFL-Jyväskylä [80] and ISAC-TRIUMF [81].

To determine the β-asymmetry parameter nuclei have to be polarised. The project is therefore being set up at the new versatile ion-polarised techniques on-line (VITO) beam line [84, 85] at ISOLDE. Optical pumping with a circularly polarised laser beam will be used to polarise the ^{35}Ar beam before it will be implanted into a suitable crystal host placed in a holding magnetic field so as to maintain the polarisation sufficiently long ($t_{1/2}(^{35}\mathrm{Ar}) = 1.78$ s). The angular distribution of the positrons emitted in the decay of polarised nuclei is given by [23]

$$W(\theta) = W_0\left(1 + \frac{v}{c}PA\cos\theta\right)$$

with W_0 the transition rate in the absence of polarisation, v/c the velocity of the positrons relative to the speed of light, P the degree of nuclear polarisation, and θ the angle between the positron momentum and the nuclear spin. With β detectors close to the $\theta = 0°$ and 180° positions and a reversible nuclear spin (i.e. polarisation) ($\pm J$) the experimental asymmetry $\mathcal{A}$ can be defined as

$$\mathcal{A} = \left\langle \frac{v}{c}\cos\theta \right\rangle PA = \frac{R-1}{R+1}$$

with

$$R = \sqrt{\frac{N(0, +J)N(\pi, -J)}{N(0, -J)N(\pi, +J)}}$$

and where $N(\theta, \pm J)$ are the numbers of counts at angle θ for each nuclear spin direction. The factor $\left\langle \frac{v}{c}\cos(\theta) \right\rangle$ takes into account the kinematic and geometrical factors and can be

determined at the 1%–2% level of precision with state-of-the-art Monte Carlo calculations (see e.g. [36]). As this is not enough to reach the required 0.5% precision on the asymmetry parameter A the method previously employed in [86, 87] will be used, which measured the ratio of the experimental β asymmetry for the mirror β transition to the ^{35}Cl ground state relative to the asymmetry of the $3/2^+ \rightarrow 1/2^+$ pure GT transition to the first-excited state (at an excitation energy of 1.22 MeV) with an endpoint energy of 3.725 MeV and a branching ratio of 1.23%:

$$\frac{A_{\mathrm{gs}}}{A_{\mathrm{ex}}} = \frac{\left\langle \frac{v}{c}\cos\theta \right\rangle_{\mathrm{ex}} \mathcal{A}_{\mathrm{gs}}}{\left\langle \frac{v}{c}\cos\theta \right\rangle_{\mathrm{gs}} \mathcal{A}_{\mathrm{ex}}}.$$

As the nuclear spin polarisation P cancels out from this ratio and $A_{\mathrm{ex}} = 1$, the precision on the asymmetry parameter for the mirror β transition, A_{gs}, will depend on the statistical and systematic errors on the two experimental asymmetries, $\mathcal{A}_{\mathrm{gs}}$, and $\mathcal{A}_{\mathrm{ex}}$, and on the precision on the calculated ratio of the kinematical and geometrical factors. Contrary to the absolute value for each individual factor, the ratio of the two factors can easily be determined in simulations with a precision well below the required 0.5%.

Because the branching ratio of the β transition to the first excited state is only 1.23%, the precision on A_{gs} will be limited by the statistical and systematic error on $\mathcal{A}_{\mathrm{ex}}$. The experimental apparatus will therefore be designed so as to maximise the efficiency for detecting coincidence events between the positrons and the 1.22 MeV γ rays signalling the population of the first excited state. A $\beta\gamma$-coincidence setup including two plastic scintillation β detectors and up to 24 CsI scintillators for detecting γ rays is being considered for this. Monte Carlo simulations have shown that the 0.5% statistical precision on A_{gs} can be achieved within a few days of beam time with about 10^6 decays per second for the implanted ^{35}Ar and a nuclear polarisation, P, between 20% and 30% [46].

In the planned measurements ^{35}Ar ions from a nanostructured CaO target will be neutralised with K vapour in a charge exchange cell. About 30%–40% of the neutral Ar will end up in the metastable $(3p^5 4s[3/2])_2$ state at about 11.6 eV which can be polarised via optical pumping with 811 nm circularly polarised laser light to the $(3p^5 4p[5/2])_3$ state. Multi-frequency pumping between the different hyperfine levels of the two states involved will be used to almost fully polarise the Ar atoms in the metastable state. A holding field along the beam line will maintain the atomic polarisation. Other Ar I fine structure levels around 11 eV excitation energy will also be populated in the charge exchange process, but these will not be affected by the optical pumping. Thus, these unpolarised atoms will reduce the final nuclear spin polarisation of the Ar atom beam to a maximum of 30%–40%. In a second phase of the project it is envisaged to re-ionise the polarised part of the beam and separate it from the atomic (non-polarised) beam. This could be achieved either by state-selective collisional re-ionisation, or by laser ionisation with a pulsed laser, as is e.g. already done in the collinear resonant ionisation spectroscopy technique at ISOLDE [47]. A potential increase of the polarisation by roughly a factor of 2 is anticipated. However, the viability of state-selective collisional re-ionisation for ^{35}Ar is still to be explored (a re-ionising gas target will be installed at the VITO beam line for this), while for laser re-ionisation an appropriate scheme will have to be identified and the efficiency of this process is to be investigated as well.

In the summer of 2016 the first stage of the laser polarisation setup, including a charge exchange cell, acceleration–deceleration electrodes to Doppler-tune the energy of the ions into resonance with the laser light for optical pumping, a deflector to separate the non-neutralised ions from the atom beam, a photomultiplier to detect the fluorescence of the

polarised beam, an optical-pumping section and, finally, an implantation chamber and two β detectors between the poles of a NMR magnet were installed and commissioned. Polarisation tests were performed with the isotopes ^{26}Na ($t_{1/2} = 1.1$ s) and ^{28}Na ($t_{1/2} = 30$ ms) which can be well polarised as neutral atoms using the D_2 transition and for which large β asymmetries had previously been observed in a NaF crystal at room temperature [88]. Polarisations of 28% for ^{26}Na and 59% for ^{28}Na were observed [89] in agreement with the earlier observations of [88]. In a next phase the laser scheme for polarising ^{35}Ar will be tested and the implantation crystal selected. Simultaneously, the $\beta\gamma$-coincidence setup will be developed as well.

3. Probing scalar and tensor currents in the β decay of radioactive nuclei

3.1. The β asymmetry parameter in the decay of polarised ^{67}Cu

Tensor type charged weak currents in nuclear β decay are 'traditionally' probed in $\beta\nu$-correlation measurements (e.g. [29, 90]). However, when nuclei are polarised also a measurement of the angular distribution (viz asymmetry) of the emitted β particles can be used for this. The presence of the NICOLE low-temperature nuclear orientation setup [91] on-line coupled to the ISOLDE facility offers the unique possibility to perform such measurements with short-lived radioactive isotopes. In addition, the dependence of the β-asymmetry parameter, A, on the coupling constants for a tensor type weak interaction, i.e. C_{T} and C'_{T}, is primarily linear, whereas the $\beta\nu$-correlation coefficient, a, has a quadratic dependence [7, 23]. Both types of measurements therefore provide complementary results.

Earlier β-asymmetry parameter measurements had already been performed in Leuven and at ISOLDE to determine small isospin-mixing effects in $J^\pi \rightarrow J^\pi$ mixed Fermi to GT β transitions caused by the electromagnetic interaction [92–94]. These have shown how the precision could further be improved, as was required to search for charged weak tensor currents in $J \rightarrow J - 1$ pure GT transitions. Neglecting terms quadratic in the tensor coupling constants and assuming maximal parity violation for the vector and axial-vector weak currents as well as time-reversal invariance [95, 96], the β-asymmetry parameter for such transitions can be written as [23, 28]

$$\widetilde{A}_{\mathrm{GT}} \equiv \frac{A}{1 \pm \langle \frac{m}{E_{\mathrm{e}}} b \rangle} \simeq A\left[1 \mp \frac{\gamma m}{E_{\mathrm{e}}} \mathrm{Re}\left(\frac{C_{\mathrm{T}} + C'_{\mathrm{T}}}{C_{\mathrm{A}}}\right)\right], \tag{1}$$

with the dependence on tensor couplings coming from the GT part of the Fierz interference term, b.

To polarise nuclei the NICOLE setup makes use of the low-temperature nuclear orientation method [40, 41]. For this nuclei are embedded into an iron foil that is soldered onto the Cu sample holder of a ^{3}He–^{4}He dilution refrigerator and cooled to temperatures in the millikelvin region in the presence of a magnetic field. The nuclear polarisation is obtained by the magnetic dipole interaction between this field and the magnetic moment of the nuclei. The β-asymmetry parameter, $\tilde{A}$, is then extracted from the observed angular distribution of the β particles

$$W(\theta) = 1 + f\frac{v}{c}\tilde{A}PQ\cos\theta. \tag{2}$$

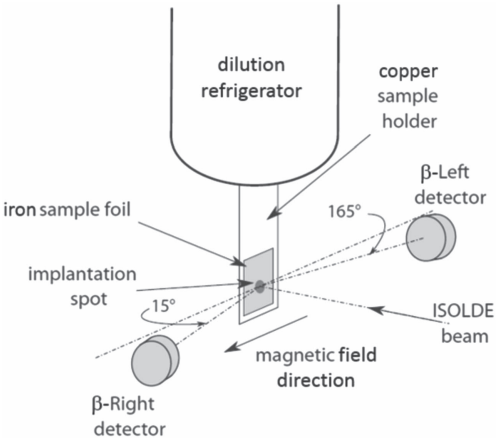

Figure 8. Schematic view of the β-particle detectors in the NICOLE dilution refrigerator setup at ISOLDE, CERN. The iron sample foil was soldered onto the copper sample holder and cooled to temperatures as low as 8 mK to polarise the ^{67}Cu nuclei. The incoming radioactive beam from ISOLDE is perpendicular to the sample foil. The right (left) particle detectors were directly facing the sample foil, containing the implanted nuclei, at an angle of 15° (165°) to minimise the effect of scattering in the foil. Adapted figure with permission from [104]. Copyright (2014) by the American Physical Society.

Here f is a quality factor indicating which fraction of nuclei feels the full orienting hyperfine interaction [97, 98], v/c is the β particle's initial velocity relative to the speed of light, P the degree of nuclear polarisation, the factor Q takes into account the solid angle as well as effects of the magnetic field and scattering, while θ is the angle of emission of the β particle with respect to the magnetisation (nuclear polarisation) direction in the Fe foil.

In order to take into account the effect of the magnetic field on the β particles' trajectory, as well as of (back)scattering in the source foil, on the detector and on surrounding materials, all of which modify the value of the solid angle correction factor, Q, extensive use was made of simulations based on the Geant4 package [33]. For this the code had first been optimised for dealing with β particles with energies in the tens of keV to few MeV range, showing good performance at the few-percent level [35, 36, 99], in line with recent work from other authors (see e.g. [100–103]).

Two β-asymmetry measurements had already been performed off-line on the pure GT transitions of ^{114}In [27] and ^{60}Co [28], both showing good agreement with the Standard Model values at the 1.5% and 2.0% relative precision on $\widetilde{A}_{\mathrm{GT}}$ that was obtained, respectively. A third measurement was performed at ISOLDE with ^{67}Cu ($t_{1/2} = 61.9$ h) obtained from the decay of ^{67}Ni nuclei ($t_{1/2} = 21$ s) that had been implanted directly into a Fe foil cooled to about 10 mK inside the NICOLE setup [104]. The rather low β-endpoint energy of 562 keV for ^{67}Cu enhances the sensitivity to tensor currents (see equation (1)). The β particles were observed with two planar high purity germanium detectors with a sensitive diameter of 16 mm and a thickness of 4 mm produced in the Nuclear Physics Institute in Řež Prague [105–107]. They were mounted inside the 4 K radiation shield of the NICOLE refrigerator to minimise energy loss and scattering effects (figure 8). Experimental angular distributions for the β particles of ^{67}Cu were obtained as $W(\theta) = N_{\mathrm{cold}}(\theta)/N_{\mathrm{warm}}(\theta)$ with $N_{\mathrm{cold,warm}}(\theta)$ the count rates in a given energy bin in the β spectrum when the sample is polarised (i.e. at

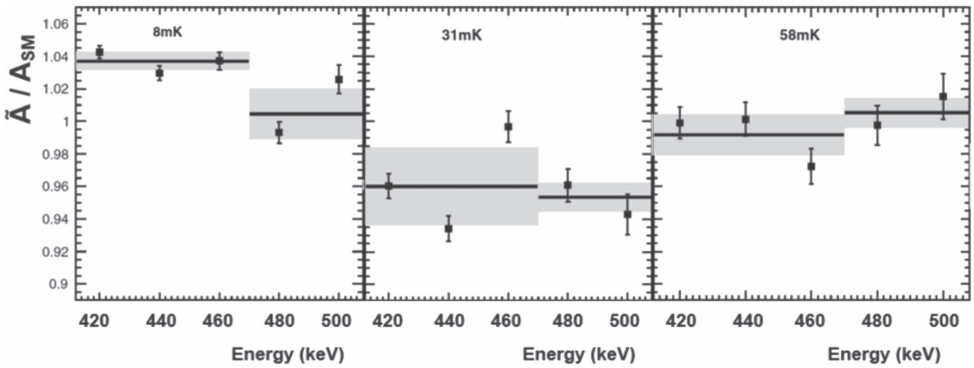

Figure 9. Ratio $\tilde{A}/A_{\mathrm{SM}}$ as a function of energy for three of the six sample temperatures (degrees of polarisation) in the ^{67}Cu experiment. Weighted averages are shown as black horizontal lines with the grey bands indicating the 1σ error bars for the regions from 410 to 470 keV (containing counts from two β branches) and from 470 to 510 keV (containing only counts from the highest-energy branch). No significant energy-dependent effects are seen, indicating that at this level of precision Geant4 is correctly taking such effects into account. Adapted figure with permission from [104]. Copyright (2014) by the American Physical Society.

millikelvin temperatures; cold) or unpolarised (i.e. at about 4.2 K; warm). A precision pulse generator was used for dead time correction.

Measurements were performed at six different temperatures (degree of polarisation) with the β spectrum being divided into five energy bins covering the energy range from 410 to 510 keV. The results for all energy bins mutually agreed within error bars (figure 9). However, as only the energy region between 470 and 510 keV (2 bins) contained only counts from the highest-energy β branch, and the branching ratios for the different β transitions in the decay of ^{67}Cu are not known with sufficient precision, the energy region below 470 keV was not used for the final analysis. For normalisation purposes an on-line measurement of the β asymmetry of ^{68}Cu was finally performed as well. The experimental result, $\tilde{A} = 0.584(13)$ [104] is systematics limited with the dominant systematic error being related to the precision on the half-life and the precision with which the degree of nuclear polarisation could be obtained. The value obtained agrees with the Standard Model value of 0.5993(2) (which takes into account recoil corrections [104]) and corresponds to $-0.023 < (C_{\mathrm{T}} + C'_{\mathrm{T}})/C_{\mathrm{A}} < 0.174$ (90% C.L.) for tensor type coupling constants [104]. These limits are compared to limits from other β decay experiments in figure 10.

3.2. The WITCH experiment

The WITCH experiment [42, 108–111] used a double-Penning trap combined with a retardation spectrometer to measure the energy spectrum of the recoil ions from β decays in the trapped ion cloud. The experiment was set up to search for charged scalar weak currents in the nearly pure Fermi decay of ^{35}Ar [37]. The beam from ISOLDE was transformed into bunches in the REXTRAP Penning trap [112] and pulsed down to about 100 eV above ground potential with a pulsed drift cavity [113]. The ions were then captured and cooled in a first Penning trap and finally transferred to a second one, the decay trap. Recoil ions from β decays in the latter spiralled from the strong magnetic field $B_{\mathrm{max}} = 6$ T of the Penning trap (figure 11) into the homogeneous weak field region with $B_{\mathrm{min}} = 0.1$ T in the centre of the retardation

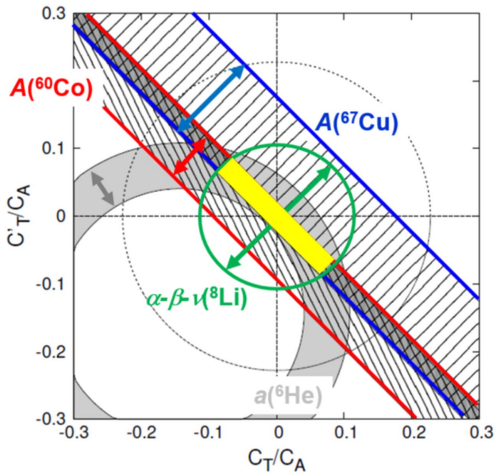

Figure 10. Limits on tensor coupling constants C_T, C_T' relative to the axial-vector coupling constant, C_A, from several $\beta\nu$ correlation and β-asymmetry parameter measurements, i.e. the $\beta\nu$ correlation of ^{6}He (grey) [90], the β–ν–α correlation in the β decay of ^{8}Li and subsequent α-particle breakup of the ^{8}Be* daughter (green circle) [30], the β-asymmetry parameter of ^{60}Co (red band) [28] and the β-asymmetry parameter of ^{67}Cu discussed here (blue band) [104]. Allowed regions are indicated by the double arrows. The common overlap between the allowed region from all four experiments is the yellow rectangular region in the centre of the graph which includes the Standard Model values $C_T = C_T' = 0$.

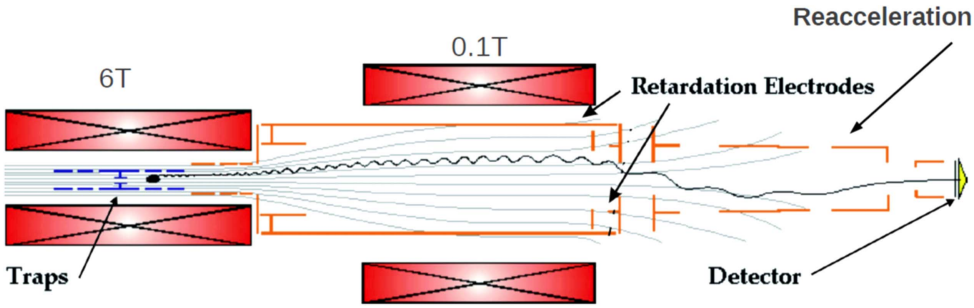

Figure 11. Schematic view of the WITCH Penning ion traps in the 6 T magnetic field, the retardation spectrometer, with the analysing plane in the centre of a 0.1 T magnet field, and the detector region. Magnetic field lines and the trajectory of a recoil ion are also shown.

spectrometer during which the energy of the ion motion perpendicular to the magnetic field lines was converted into longitudinal kinetic energy. This could then be probed in the homogeneous low field region by retarding the ions with a well-defined electrostatic potential. Ions that passed this analysis plane were re-accelerated to about 10 keV and observed with a micro-channel plate (MCP) detector [114, 115]. By varying the retardation voltage the integral recoil-ion spectrum could be measured.

After several improvements and upgrades to overcome the ion background in the system [111, 116, 117], the proof of principle was demonstrated [42] and initial

measurements performed [43]. Thereafter a high-statistics and high-resolution data set has been collected. The number of recoil ions was measured for about 20 different settings of the retardation potential and complemented by dedicated background and (effective) half-life measurements for different experimental conditions [44]. During these measurements and their subsequent analysis, previously unidentified systematic effects, including an energy-dependent efficiency of the main MCP detector and a radiation-induced time-dependent background, have been identified. The observed recoil-ion spectrum deviated significantly from its expected shape. The analysis [118] included the understanding of the different systematic effects observed, the measured efficiency of the MCP detector, and the charge state distribution of the ^{35}Cl daughter ions as measured with the LPCTrap setup at GANIL [119], and was backed with simulations using a powerful graphics card-based code for Coulomb interactions in a Penning trap [120]. However, it became clear that further understanding and treatment of the radiation-induced background requires the continuous monitoring of e.g. the actual pressure in the Penning trap region, the size of the ion cloud, the number and the spatial distribution of the ions in the cloud, etc. Monte Carlo simulations showed that reasonable assumptions about the properties of this background would indeed have precisely the effect on the extracted recoil-ion amplitudes as is observed in the present data set [44]. This background thus constitutes the limiting factor in extracting the $\beta\nu$-angular correlation coefficient for ^{35}Ar decay using the WITCH spectrometer. It was therefore decided that the spectrometer will be re-purposed for other fundamental symmetries studies in nuclear β decay, for example the experiment described in the next section.

3.3. Outlook—search for scalar currents in the β-delayed proton decay of ^{32}Ar

The $\beta\nu$ angular correlation can be studied by different means. Most of the experiments (see e.g. [79]) measure the recoil-energy distribution of the daughter nucleus and compare this experimental distribution to Monte Carlo simulations using different assumptions for the scalar-current to vector-current ratio. For the new weak-interaction studies with ^{32}Ar decay (WISARD) experiment [48], the Doppler effect on β-delayed protons will be used to study this ratio. The vector and scalar currents have different angular distributions between the two emitted leptons: angular correlations peaked at 0° for the vector current and at 180° for the scalar current. Therefore, the recoil of the daughter nucleus is basically zero on average for the latter decay, whereas it is maximum for a vector current. In a β-delayed proton emission, the protons are emitted from a moving source imposing a Doppler effect on the proton energy.

In an experiment measuring only the proton energy, this leads to a broadening of the proton peak in the case of a vector current, whereas in the case of a purely scalar current, the proton peak is much narrower. These properties have been used in two ISOLDE experiments in the 1990s. A first experiment [82] allowed determining the $\beta\nu$ angular correlation coefficient, $a_{\beta\nu}$, to be 1.00(8) in agreement with the Standard Model expectation of 1. A more sophisticated experiment a few years later [83] arrived at a value of $a_{\beta\nu} = 0.998(5)$.

The WISARD experiment [48] will measure the emitted positron and proton in coincidence (see figure 12). Positrons and protons will be detected either in the same hemisphere or in opposite hemispheres with respect to the catcher foil. Thus for a vector current, for which the positron and the neutrino are emitted preferentially in the same direction (favoured relative angle of 0°), the daughter nucleus which emits the proton has a recoil preferentially in the opposite direction. Therefore, a proton emitted in the same direction as the positron will have a reduced energy, whereas a proton emitted in the opposite direction compared to the positron will see its energy boosted by the recoil. For a scalar current, for which the positron and the neutrino are emitted preferentially in opposite directions (favoured relative angle of 180°), the

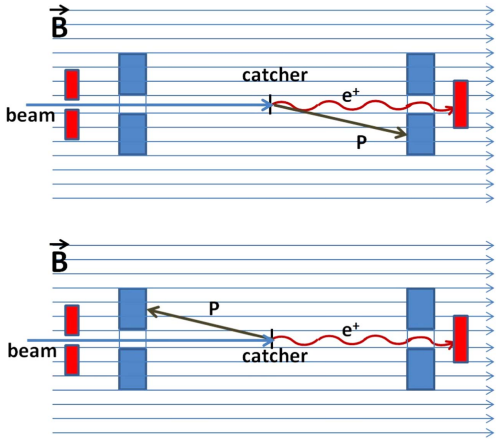

Figure 12. Schematic view of the set-up to be installed in the former WITCH magnet for the new WISARD experiment. The activity will be disposed on a thin catcher foil in the centre of the magnet. The decay positrons will spiral along the magnetic field lines towards the positron detectors (in red) on both sides of the catcher. Due to their bending radius they cannot reach the 'compact-disk'-type proton detectors (circular detector with a hole in its centre, in blue). In such a way, coincidences of positrons and protons in the same hemisphere and in opposite hemispheres can be made. All detectors will be cooled in the cold bore of the magnet.

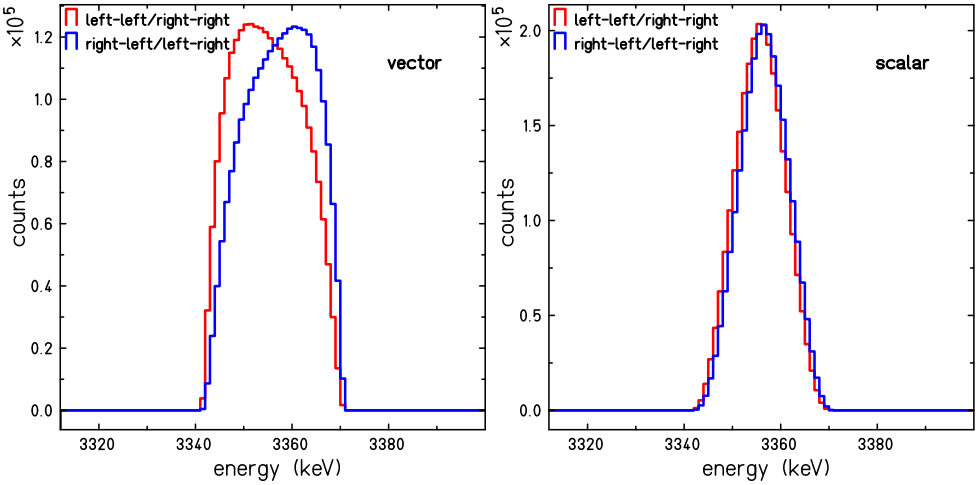

Figure 13. Monte Carlo simulations of peak shapes of the isobaric analogue state in the case of a purely vector current for the Fermi β decay (left-hand side) and a purely scalar current (right-hand side). The red curve is for a data cut where the positron and the proton are observed on the same side of the catcher, whereas the blue curve is for a detection of the two particles on opposite sides. The simulations were carried out with 10^9 ^{32}Ar decays.

average recoil of the daughter nucleus is zero. Therefore, detecting the proton and the positron in the same or in opposite hemisphere does not change the proton energy (see figure 13). Thus, instead of measuring a Doppler broadening, the WISARD experiment will measure a Doppler shift in one or the other direction which provides increased sensitivity.

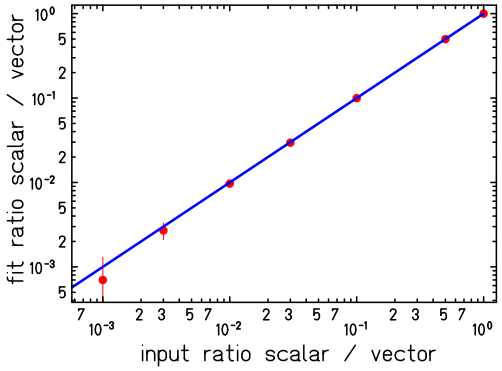

Figure 14. Plot of the fit results for different scalar-to-vector ratios as the input to the MC simulations. These results were obtained with 10^9 decays. The line is the 45° diagonal.

The Monte Carlo simulations performed to study the sensitivity of the proposed experiment are shown in figure 13 for purely vector and scalar currents. These simulations do not yet include the complete transport of the particles through the magnetic field, backscattering effects etc but are only angular cuts respecting the geometrical detection efficiencies of the different detectors. However, they clearly show the effect expected if the experimental energy resolution is sufficiently good (10 keV). Simulations with a mixture of scalar and vector contributions can give indications with respect to the final precision on the correlation parameter $a_{\beta\nu}$. Figure 14 shows such a study where the scalar contribution in the decay to the isobaric analogue state (IAS) was reduced from 100% to 0.1% in the input of the simulations. The resulting shape of the IAS was fitted with freely varying contributions of scalar and vector currents. As the figure shows, the input mixing is found as the result of the fit down to 0.1%. These still relatively simple simulations will be refined in the future to include more realistic conditions in a full GEANT4 simulation.

4. Parity violation in the γ decay of ^{180m}Hf

Whereas parity violation in the weak interaction has been well established in nuclear β decay (e.g. [1, 2, 18, 121, 122]), the level to which nuclear states can or cannot be taken as eigenstates of parity has much less been documented as yet. Parity mixing in bound nuclear systems is understood as being due to weak interaction terms (viz violating parity) in the nuclear Hamiltonian. The strongest evidence for parity non-conservation in nuclear states is the observed presence of an irregular $E2/M2$ mixing in the $8^- \rightarrow 6^+$ 501 keV γ decay of the 5.5 h ^{180m}Hf state [123] (and references therein). Parity mixing arises here because of the proximity in energy ($\Delta E = 57$ keV) of the two spin $I = 8$ states ($\Delta E = 57$ keV) with opposite parity at 1142 and 1085 keV, and is significantly enhanced due to large K-forbiddenness ($\Delta K = 8$) slowing down the 'regular' γ transitions and thereby allowing the 'irregular' components to be seen. Thus, although the parity non-conserving matrix element is rather small (i.e. about 1 meV), the total enhanced effect is unusually large. Previously [123] the 'irregular' multipole mixing ratio was measured to be $\epsilon\,(E2/M2) = -0.030(2)$, i.e. a 15 standard deviations parity violating effect. The validity of this result was verified [45] at ISOLDE making use of highly improved source making methods, but also of the higher degrees of polarisation and much longer continuous observation times that could be achieved

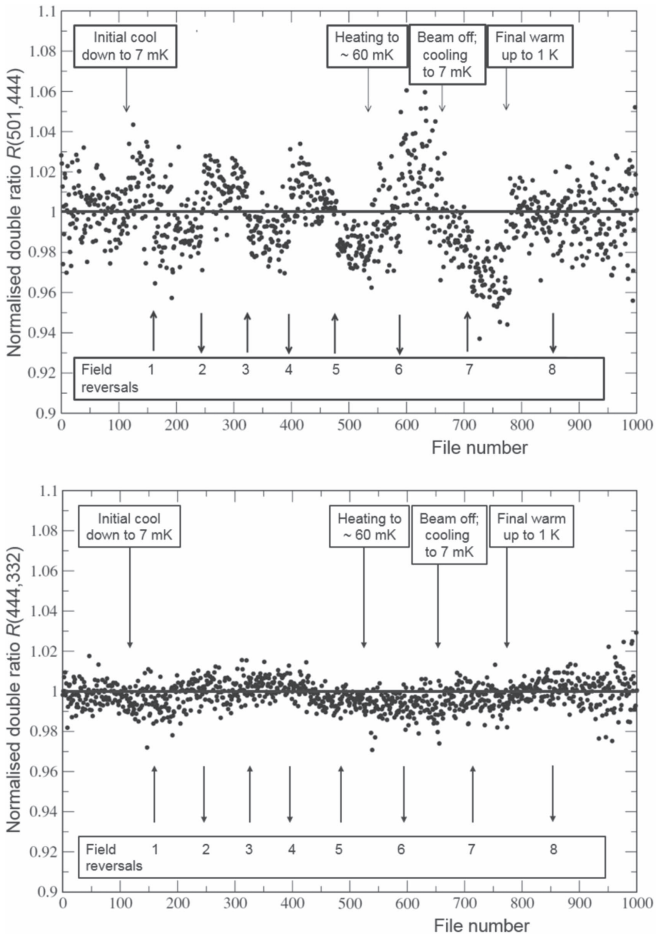

Figure 15. Double ratio $R(\gamma 1/\gamma 2)$ of counts (equation (4)) measured in the left and right on-axis detectors for all files of the experiment and normalised to the average pre-cooldown (i.e. warm, non-oriented) value of R for the files 7386. (a) $R(501/444)$, showing clearly the parity-violating asymmetry in the γ ray count rate ratio which consistently changes sign when the magnetic field direction is reversed. (b) $R(444/332)$, showing no correlation which the magnetic field reversals. Reprinted with permission from [45]. Copyright 2007 by the American Physical Society.

within the NICOLE low temperature nuclear orientation setup in comparison to the previous result [123].

If either of the nuclear states between which a γ decay occurs are not eigenstates of parity, odd terms in cos θ occur in the angular distribution. These are most clearly seen in the asymmetry $\mathcal{A}(T)$ defined as [123]

$$\mathcal{A}(T) = 2\frac{W(0^\circ, T) - W(180^\circ, T)}{W(0^\circ, T) + W(180^\circ, T)} \propto \frac{P_{\text{odd}}}{1 + P_{\text{even}}}, \tag{3}$$

where $W(\theta, T) = N(\theta, T)/N(\theta, \text{unpol})$, with $N(\theta, T)$ and $N(\theta, \text{unpol})$ the count rate at angle θ, respectively, at a temperature T and for unpolarised nuclei, and with $P_{\text{odd/even}}$ the parity-odd, respectively parity-even, contributions to the angular distribution. The asymmetry

effect shows up easily in the double ratio

$$\mathcal{R}(501,\,444) = \frac{N(501,\,0^\circ)/N(444,\,0^\circ)}{N(501,\,180^\circ)/N(444,\,180^\circ)}\,, \tag{4}$$

with the 501 keV γ transition the one showing appreciable asymmetry and the 444 keV transition being a symmetric one. During intervals of stable and high nuclear polarisation, and when the implanted beam was stable as well, the magnetic field was regularly reversed showing a clearly correlated change in the ratio $\mathcal{R}(501,\,444)$, changing between about 0.97 and 1.03 (figure 15), with no change in the ratio $\mathcal{R}(444,\,332)$ containing two symmetric transitions [45]. For the 501 keV transition values for the asymmetry $\mathcal{A}(T)$ ranging from $-0.93(13)\%$ to $-1.48(26)\%$ were observed at temperatures between 7.6(1) mK and 57(7) mK, with $\mathcal{A}(T) = +0.11(18)\%$ for an unpolarised sample. For the symmetric 215 keV, 332 keV and 444 keV γ transitions, no non-zero asymmetries were observed with the values averaged over all temperatures being, respectively $\mathcal{A}(T) = -0.04(7)\%$, $-0.07(5)\%$ and $-0.03(8)\%$ [45]. The asymmetry for the 501 keV transition, moreover, showed the expected temperature variation predicted by the earlier result but now taken to significantly higher degrees of nuclear polarisation, leading to the final value $\epsilon = -0.0324(16)(19)$ for the irregular $E2/M2$ mixing ratio [45], in extremely close agreement with the previous result $-0.030(2)$ [123]. This asymmetry is currently the best established demonstration of parity admixture in nuclear phenomena. Unfortunately, to date effective theoretical calculations trying to provide understanding of this result are prevented by the specific nuclear structure of the levels involved, notably the high degree of K forbiddeness of the $8^- \rightarrow 6^+$ decay.

5. Conclusion

It is clear that the ISOLDE facility, providing a wide range of isotopes of different nuclear states, has significantly contributed to furthering progress in the understanding of the symmetries as well as the structure and properties of the weak interaction, and will continue to do so. Indeed, a wide range of mainly precision measurements have been performed over the last decade or so ranging from half-lives, branching ratios and nuclear masses relevant for the determination of the V_{ud} quark-mixing matrix element, over β-asymmetry and $\beta\nu$ correlation measurements searching for possible tensor and/or scalar contributions to the weak interaction, up to a measurement showing the effect of parity violation in the weak interaction in γ decay. Further, several new projects, respectively, searching for charged scalar currents in the β-delayed proton decay of ^{32}Ar or trying to determine the V_{ud} quark-mixing matrix element from the β-asymmetry parameter in the mirror decay of ^{35}Ar, have just started and will, together with new measurements contributing to the corrected $\mathcal{F}t$ values for the $0^+ \rightarrow 0^+$ and mirror β transitions, undoubtedly provide additional important information on the nature of the weak interaction in the years to come.

References

[1] Wu C S *et al* 1957 *Phys. Rev.* **105** 1413
[2] Chirovsky L M *et al* 1984 *Nucl. Instrum. Methods Phys. Res.* **219** 103
[3] Goldhaber N D, Grodzins L and Sunyar A W 2012 *Phys. Rev.* **109** 1015
[4] Allen J S *et al* 1959 *Phys. Rev.* **116** 134
[5] Hardy J C and Towner I S 2015 *Phys. Rev.* C **91** 025501
[6] Herczeg P 2001 *Prog. Part. Nucl. Phys.* **46** 413
[7] Severijns N, Beck M and Naviliat-Cuncic O 2006 *Rev. Mod. Phys.* **78** 991

[8] Severijns N and Naviliat-Cuncic O 2011 *Annu. Rev. Nucl. Part. Sci.* **61** 23
[9] Hardy J C and Towner I S 2013 *Ann. Phys. (Berlin)* **525** 443
[10] Severijns N and Naviliat-Cuncic O 2013 *Phys. Scr.* **T152** 014018
[11] Naviliat-Cuncic O and González-Alonso M 2013 *Ann. Phys. (Berlin)* **525** 600
[12] Wauters F, García A and Hong R 2014 *Phys. Rev.* C **89** 025501
[13] Cirigliano V, Gardner S and Holstein B R 2013 *Progr. Part. Nucl. Phys.* **71** 93
[14] Holstein B R 2015 *J. Phys. G: Nucl. Part. Phys.* **41** 114001
[15] Vos K, Wilschut H W and Timmermans H G E 2015 *Rev. Mod. Phys.* **87** 1483
[16] Nico J 2009 *J. Phys. G: Nucl. Part. Phys.* **36** 104001
[17] Dubbers D and Schmidt M G 2011 *Rev. Mod. Phys.* **83** 1111
[18] Thomas E *et al* 2001 *Nucl. Phys.* A **694** 559
[19] Bhattacharya T *et al* 2012 *Phys. Rev.* D **85** 054512
[20] Cirigliano V, González-Alonso M and Graesser M L 2013 *J. High Energ. Phys.* JHEP02 (2013)046
[21] Profumo S, Ramsey-Musolf M J and Tulin S 2007 *Phys. Rev.* D **75** 075017
[22] Ramsey-Musolf M J and Su S 2008 *Phys. Rep.* **456** 1
[23] Jackson J D, Treiman S B and Wyld H W Jr 1957 *Phys. Rev.* **106** 517
Jackson J D, Treiman S B and Wyld H W Jr. 1957 *Nucl. Phys.* **4** 206
[24] Adelberger E *et al* 1999 *Phys. Rev. Lett.* **83** 1299
Adelberger E *et al* 1999 *Phys. Rev. Lett.* **83** 3101 (erratum)
[25] Gorelov A *et al* 2005 *Phys. Rev. Lett.* **94** 142501
[26] Vetter P A, Abo-Shaeer J R, Freedman S J and Maruyama R 2008 *Phys. Rev.* C **77** 035502
[27] Wauters F *et al* 2009 *Phys. Rev.* C **80** 062501(R)
[28] Wauters F *et al* 2010 *Phys. Rev.* C **82** 055502
[29] Fléchard X *et al* 2011 *J. Phys. G: Nucl. Part. Phys.* **38** 055101
[30] Sternberg M G *et al* 2015 *Phys. Rev. Lett.* **115** 182501
[31] Behr J and Gwinner G 2009 *J. Phys. G: Nucl. Part. Phys.* **36** 033101
[32] Blaum K 2006 *Phys. Rep.* **425** 1
[33] Agostinelli S *et al* (GEANT Collaboration) 2003 *Nucl. Instrum. Methods Phys. Res.* A **506** 250
[34] Rodriguez D *et al* 2000 *Eur. Phys. J.* A **42** 397
[35] Wauters F *et al* 2009 *Nucl. Instrum. Methods Phys. Res.* A **609** 156
[36] Soti G *et al* 2013 *Nucl. Instrum. Methods Phys. Res.* A **728** 11
[37] Severijns N, Tandecki M, Phalet T and Towner I S 2008 *Phys. Rev.* C **78** 055501
[38] Naviliat-Cuncic O and Severijns N 2009 *Phys. Rev. Lett.* **102** 142302
[39] Blaum K *et al* 2003 *J. Phys. B: At. Mol. Opt. Phys.* **36** 921
[40] Postma H and Stone N J (ed) 1986 *Low-Temperature Nuclear Orientation* (Amsterdam: North-Holland)
[41] Wouters J *et al* 1990 *Hyperfine Interact.* **59** 59
[42] Beck M *et al* 2011 *Eur. Phys. J.* A **47** 45
[43] Van Gorp S *et al* 2014 *Phys. Rev.* C **90** 025502
[44] Finlay P *et al* 2016 *Eur. Phys. J.* A **52** 206
[45] Stone J R *et al* 2007 *Phys. Rev.* C **76** 025502
[46] Velten P 2014 *Measurement of the β-asymmetry parameter in ^{35}Ar decay with a laser polarized beam, proposal* CERN-INTC-2014-062 (INTC-P-426)
[47] de Groote R P *et al* 2015 *Phys. Rev. Lett.* **115** 132501
[48] Blank B 2016 *WISARD: weak-interaction studies with ^{32}Ar decay, letter of intent* CERN-INTC-2016-050 (INTC-I-172)
[49] Olive K A and Particle Data Group 2014 *Chin. Phys.* C **38** 090001
[50] Baessler S, Bowman J D, Penttilä S and Pocanic D 2014 *J. Phys. G: Nucl. Part. Phys.* **41** 114003
[51] Pocanic D, Frlez E and van der Schaaf A 2014 *J. Phys. G: Nucl. Part. Phys.* **41** 114002
[52] Young A R *et al* 2014 *J. Phys. G: Nucl. Part. Phys.* **41** 114007
[53] Audi G, Bersillon O, Blachot J and Wapstra A H 2003 *Nucl. Phys.* A **729** 3
[54] Marciano W J 2011 *J. Phys.: Conf. Ser.* **312** 102002
[55] Herfurth F *et al* 2001 *Phys. Rev. Lett.* **87** 142501
[56] Helmer R G *et al* 2003 *Nucl. Instrum. Methods Phys. Res.* A **511** 360
[57] Blank B *et al* 2014 *Nucl. Instrum. Methods Phys. Res.* A **776** 34
[58] Blank B *et al* 2010 *Eur. Phys. J.* A **44** 363
[59] Delahaye P, Blank B and Sturm S 2008 *Nucl. Instrum. Methods Phys. Res.* B **266** 4647

[60] Park H I *et al* 2011 *Phys. Rev.* C **84** 065502
[61] Blank B *et al* 2014 *Eur. Phys. J.* A **51** 8
[62] Park H I *et al* 2014 *Phys. Rev. Lett.* **112** 102502
[63] Delahaye P *et al* 2015 private communication
[64] Kurtukian Nieto T K *et al* 2017 *J. Phys. G: Nucl. Part. Phys.* accepted
[65] Shidling P D *et al* 2014 *Phys. Rev.* C **90** 032501
[66] Savard G *et al* 1995 *Phys. Rev. Lett.* **74** 1521
[67] Fujikawa B *et al* 1999 *Phys. Lett.* B **449** 6
[68] George S *et al* 2008 *Eur. Phys. Lett.* **82** 50005
[69] Kellerbauer A *et al* 2004 *Phys. Rev. Lett.* **93** 072502
[70] Blaum K 2004 *Progress report for experiment IS413* CERN-INTC-2004-020 (INTC-SR-002)
[71] Mukherjee M *et al* 2004 *Phys. Rev. Lett.* **93** 150801
[72] Herfurth F *et al* 2002 *Eur. Phys. J.* A **15** 17
[73] George S *et al* 2007 *Phys. Rev. Lett.* **98** 162501
[74] Blaum K *et al* 2003 *Phys. Rev. Lett.* **91** 260801
[75] Wrede C *et al* 2010 *Phys. Rev.* C **81** 055503
[76] Kankainen A *et al* 2010 *Phys. Rev.* C **82** 052501
[77] Bhattacharya M *et al* 2008 *Phys. Rev.* C **77** 065503
[78] Mukherjee M *et al* 2008 *Eur. Phys. J.* A **35** 31
[79] Rodrguez D *et al* 2006 *Nucl. Instrum. Methods Phys. Res.* A **565** 876
[80] Eronen T 2013 *Q-Value measurements of mirror transitions for fundamental interaction studies, JYFL proposal* I189
[81] Finlay P *et al* 2011 Proposal for experiment S1517 to the TRIUMF EEC (https://mis.triumf.ca/science/experiment/view/S1517)
[82] Schardt D and Riisager K 1993 *Z. Phys.* A **345** 265
[83] Adelberger E G *et al* 1999 *Phys. Rev. Lett.* **83** 1299
[84] Deicher M 2013 *VITO—versatile ion-polarized techniques on-line at ISOLDE, letter of intent* CERN-INTC-2013-013 (INTC-O-017)
[85] Garcia Ruiz R F *et al* 2015 *EPJ Web Conf.* **93** 07004
[86] Garnett D *et al* 1988 *Phys. Rev. Lett.* **60** 499
[87] Converse A *et al* 1993 *Phys. Lett.* B **304** 60
[88] Keim M *et al* 2000 *Eur. Phys. J.* A **1** 31
[89] Kowalska M *et al* 2017 *J. Phys. G: Nucl. Part. Phys.* accepted
[90] Johnson C H, Pleasonton F and Carlson T A 1963 *Phys. Rev.* **132** 1149
[91] Schlösser K *et al* 1988 *Hyperfine Interact* **43** 139
[92] Schuurmans P *et al* 2000 *Nucl. Phys.* A **672** 89
[93] Severijns N *et al* 2005 *Phys. Rev.* C **71** 064310
[94] Golovko V V 2005 *PhD Thesis* Katholieke Universiteit Leuven
[95] Huber R *et al* 2003 *Phys. Rev. Lett.* **90** 202301
[96] Kozela A *et al* 2012 *Phys. Rev.* C **85** 045501
[97] van Walle E, Vandeplassche D, Wouters J, Severijns N and Vanneste L 1986 *Phys. Rev.* B **34** 2014
[98] Severijns N *et al* 2009 *Phys. Rev.* C **79** 064322
[99] Wauters F 2009 *PhD Thesis* Katholieke Universiteit Leuven
[100] Martin J W *et al* 2003 *Phys. Rev.* C **68** 055503
[101] Martin J W *et al* 2003 *Phys. Rev.* C **73** 015501
[102] Kadri O *et al* 2007 *Nucl. Instrum. Methods Phys. Res.* B **258** 381
[103] Elles S, Ivanchenko V N, Maire M and Urban L 2008 *J. Phys.: Conf. Ser.* **102** 012009
[104] Soti G *et al* 2014 *Phys. Rev.* C **90** 035502
[105] Vénos D *et al* 2000 *Nucl. Instrum. Methods Phys. Res.* A **454** 403
[106] Zákoucý D *et al* 2004 *Nucl. Instrum. Methods Phys. Res.* A **520** 80
[107] Wauters F *et al* 2009 *Nucl. Instrum. Methods Phys. Res.* A **604** 563
[108] Beck M *et al* 2003 *Nucl. Instrum. Methods Phys. Res.* A **503** 567
[109] Beck M *et al* 2003 *Nucl. Instrum. Methods Phys. Res.* B **204** 521
[110] Kozlov V Y *et al* 2004 *Phys. At. Nucl.* **67** 1112
[111] Kozlov V Y *et al* 2006 *Int. J. Mass. Spec.* **251** 159
[112] Ames F *et al* 2005 *Nucl. Instrum. Methods Phys. Res.* A **538** 17
[113] Coeck S *et al* 2007 *Nucl. Instrum. Methods Phys. Res.* A **572** 585

[114] Liénard E *et al* 2005 *Nucl. Instrum. Methods Phys. Res.* A **551** 375
[115] Coeck S *et al* 2006 *Nucl. Instrum. Methods Phys. Res.* A **557** 516
[116] Kozlov V *et al* 2008 *Nucl. Instrum. Methods Phys. Res.* B **266** 4515
[117] Tandecki M *et al* 2011 *Nucl. Instrum. Methods Phys. Res.* A **629** 396
[118] Porobic T 2015 *PhD Thesis* Katholieke Universiteit Leuven
[119] Couratin C *et al* 2013 *Phys. Rev.* A **88** 041403(R)
[120] Van Gorp S *et al* 2011 *Nucl. Instrum. Methods Phys. Res.* A **638** 192
[121] Severijns N *et al* 1993 *Phys. Rev. Lett.* **70** 4047
[122] Severijns N *et al* 1994 *Phys. Rev. Lett.* **73** 611 (erratum)
[123] Chou T S, Krane K S and Shirley D A 1975 *Phys. Rev.* C **12** 286